

Synthesis of long-chain amide analogs of the cannabinoid CB1 receptor antagonist *N*-(piperidinyl)-5-(4-chlorophenyl)-1-(2,4-dichlorophenyl)-4-methyl-1*H*-pyrazole-3-carboxamide (SR141716) with unique binding selectivities and pharmacological activities

Brian F. Thomas,^{a,*} Ma. Elena Y. Francisco,^a Herbert H. Seltzman,^a
James B. Thomas,^a Scott E. Fix,^a Anne-Kathrin Schulz,^a Anne F. Gilliam,^a
Roger G. Pertwee^b and Leslie A. Stevenson^b

^aScience and Engineering Group, Research Triangle Institute, Research Triangle Park, NC 27709, USA

^bDepartment of Biomedical Sciences, Institute of Medical Sciences, University of Aberdeen, Foresterhill, Aberdeen AB25 2ZD, Scotland, UK

Received 18 November 2004; revised 31 May 2005; accepted 1 June 2005

Available online 1 July 2005

Abstract—An extended series of alkyl carboxamide analogs of *N*-(piperidinyl)-5-(4-chlorophenyl)-1-(2,4-dichlorophenyl)-4-methyl-1*H*-pyrazole-3-carboxamide (SR141716; **5**) was synthesized. Each compound was tested for its ability to displace the prototypical cannabinoid ligands (³H]CP-55,940, [³H]2; [³H]SR141716, [³H]5; and [³H]WIN55212-2, [³H]3), and selected compounds were further characterized by determining their ability to affect guanosine 5'-triphosphate (GTP)-γ-[³⁵S] binding and their effects in the mouse vas deferens assay. This systematic evaluation has resulted in the discovery of novel compounds with unique binding properties at the central cannabinoid receptor (CB1) and distinctive pharmacological activities in CB1 receptor tissue preparations. Specifically, compounds with nanomolar affinity which are able to fully displace [³H]5 and [³H]2, but unable to displace [³H]3 at similar concentrations, have been synthesized. This selectivity in ligand displacement is unprecedented, in that previously, compounds in every structural class of cannabinoid ligands had always been shown to displace each of these radioligands in a competitive fashion. Furthermore, the selectivity of these compounds appears to impart unique pharmacological properties when tested in a mouse vas deferens assay for CB1 receptor antagonism.

© 2005 Published by Elsevier Ltd.

1. Introduction

There have been at least two types of cannabinoid receptors characterized to date, CB1¹ and CB2.² CB1 receptors are found primarily in brain and neuronal tissue, while CB2 receptors are found predominantly in immune cells and tissues. Both are G-protein-coupled receptors,³ sharing approximately 48% homology in their amino acid sequences,⁴ and both responding to ligand binding through coupling with mitogen-activated protein kinase⁵ and adenylyl cyclase.⁶ Other signal transduction pathways have been demonstrated for

these receptors. For example, CB1 receptors are also coupled to several types of potassium^{7,8} and calcium channels,⁹ and thereby inhibit the release of several neurotransmitters.^{10–13} Despite the euphoria production and 'high' associated with agonists at the CB1 receptor, these compounds have therapeutic utility as antiglaucoma agents, antiemetics or appetite stimulants, and therapeutic potential as analgesics, or for the treatment of symptoms of multiple sclerosis, and other indications. Agonists at the CB2 receptor may hold promise as immunomodulators.¹⁴ Similarly, CB1 antagonists are being investigated for their therapeutic utility in treating obesity and improving memory.¹⁵

In addition to binding the naturally occurring cannabinoids such as Δ⁹-THC (**1**), the CB1 and CB2 receptors can bind other structural classes of compounds, including nonclassical cannabinoids (CP55940, **2**), aminoalky-

Keywords: Cannabinoid; Ligand-receptor; Binding; Structure-activity relationships; CB1; Antagonist.

* Corresponding author. Tel.: +1 9195416552; fax: +1 9195416499; e-mail: bft@rti.org

lindoles (WIN55212-2, **3**), arachidonylethanolamides (anandamide, **4**), and diarylpyrazoles (SR141716, **5** or SR144528, **6**; Fig. 1). It has been suggested that all of these compounds interact as competitive ligands at a common or overlapping/interacting binding region on the CB1 receptor, since heterologous displacement curves have consistently been demonstrated between these various ligand classes.¹⁶ Indeed, overlapping superposition models have been hypothesized by several investigators for nonclassical and classical cannabinoids,^{17,18} arachidonylethanolamides and classical cannabinoids,^{19–22} aminoalkylindoles and classical cannabinoids,^{23–26} and diarylpyrazole antagonists and classical cannabinoid agonists,^{16,27} and finally, a superposition strategy for nonclassical, aminoalkylindole and classical cannabinoids has been described.¹⁶

While these superpositions represent reasonable hypotheses, in 1998, our laboratory had noted differences in the ability of a variety of compounds to compete for the rat brain CB1 receptor site when labeled with [³H]**5** as compared to when the site was labeled with [³H]**2**.²⁷ For example, the affinity of **2** differed by more than 38-fold depending on what radioligand was used to determine its K_i . WIN55212-2 (**3**) also had a greater ability to compete for the receptor when labeled with [³H]**2** as compared to [³H]**5**. In contrast, **5** was more than 5-fold more effective when competing with [³H]**5** than when competing with [³H]**2**. We hypothesized at that time that the differences in K_i values of these compounds suggest that their mode of binding or the population of binding

sites that are being occupied by these compounds and the radioligands are significantly different.

More recently, we published on a series of amide analogs of the CB1 receptor antagonist **5**.²⁸ These compounds included straight chain alkyl, hydroxy alkyl, and hydrazide analogs up to six carbons in length. Initially, we elected to characterize these compound's binding affinities at the CB1 receptor using [³H]**2** and [³H]**5**. However, during subsequent experiments with [³H]**3** in rat brain CB1 (rCB₁) preparations, subtle differences were noted in the displacement curves obtained with the three radioligands. This observation led to the synthesis of alkyl side-chain analogs of even greater length. Furthermore, we examined the binding profiles of these compounds in cells transfected with the human CB1 receptor and in human brain preparations. It was found that these compounds clearly possess unique binding selectivities, particularly in human CB1 receptor (hCB₁) preparations, representing the first clear demonstration of nonhomologous displacement curves between these three radioligands. Specifically, some long-chain alkyl amide analogs can displace [³H]**5** and [³H]**2** with reasonably high affinity, but are unable to displace [³H]**3**. The demonstration of nonheterologous displacement curves with these radioligands agrees with previous hypotheses that **3** binds with a distinct recognition site, or in a unique manner within an overlapping recognition site, compared to **2** or **5** (as described later). By extension, the binding of the 'WIN-sparing' alkyl analogs of **5** is also unique compared to the prototype antagonist **5**. However, it remains to be determined whether this distinct mode of binding imparts unique pharmacological properties.

2. Results

2.1. CB1 receptor affinity in rat brain

All of the compounds were tested for their ability to displace [³H]**2**, [³H]**5**, and [³H]**3** in rat brain membrane preparations (Table 1, Fig. 2). The CB1 receptor binding data in rat brain for this series of analogs demonstrated that as the size of the carbon chain is increased from C4 to C5, a slight increase in binding affinity is observed, there is a modest decrease at C6, followed by a slightly greater decrease at C7. Beyond this length, there appears to be a further decrease in affinity. This pattern is not as obvious with the branched alkyl amides; however, generally the pentyl and hexyl amides demonstrated the highest affinity, with the heptyl and decyl analogs having lower affinity. In addition, the data obtained in rat brain suggested that as the carbon chain extended beyond C5 or C6, both the affinity and the ability to fully displace [³H]**3** decreased more rapidly than with [³H]**2** or [³H]**5**. In addition to these observations, characterization in mouse vas deferens studies with **3** also indicated that these compounds were pharmacologically unique (described in greater detail below), and this encouraged us to extend our observations into other CB1 receptor preparations.

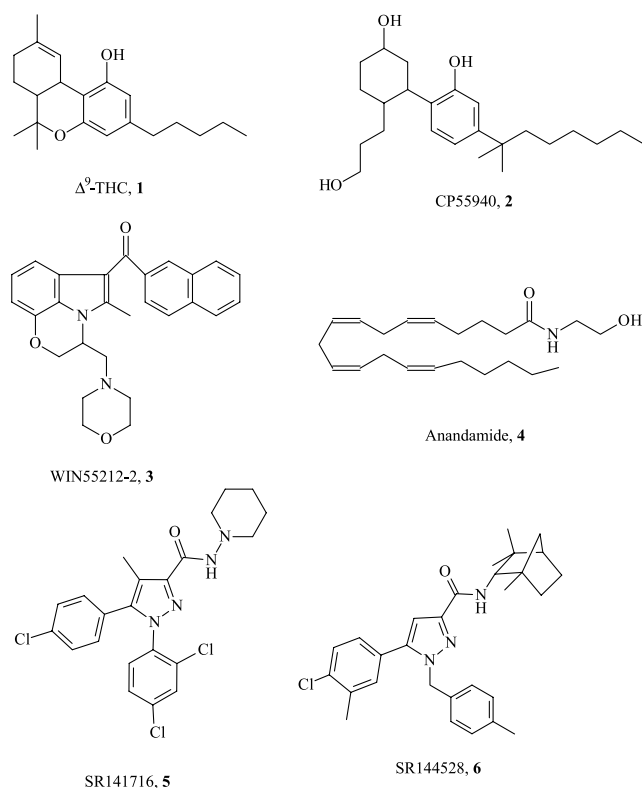


Figure 1. Structure of selected cannabinoid ligands.

Table 1. Amide analogs at the 3-position: displacement of various radioligands in whole rat brain (CB1) membrane preparations

| Compound | Substituted group | $[^3\text{H}]\mathbf{2}$ | | | $[^3\text{H}]\mathbf{5}$ | | | $[^3\text{H}]\mathbf{3}$ | | |
|-----------------------|------------------------------------|--------------------------|--------------|--------------------------|--------------------------|--------------|--------------------------|--------------------------|--------------|--------------------------|
| | | K_i (nM) | SEM | Maximum displacement (%) | K_i (nM) | SEM | Maximum displacement (%) | K_i (nM) | SEM | Maximum displacement (%) |
| 5 (SR141716) | | 6.18 | 1.2 | 86.6 | 1.18 | 0.10 | 96.5 | 1.97 | ^a | 85.7 |
| 6 (SR144528) | | 74.1 | 11.4 | 84.7 | 81.7 | 19.3 | 68.6 | | | |
| 8^b | <i>N</i> -(1-Cyclohexyl) | 2.46 | 0.10 | 96.1 | 1.07 | 0.13 | 100 | 2.23 | 0.15 | −92.6 |
| 9^b | <i>N</i> -(1-Butyl) | 13.4 | 1.0 | 91.9 | 12.8 | 4.5 | 100 | 32.8 | 26.0 | 90.8 |
| 10^b | <i>N</i> -(1-Pentyl) | 11.4 | 0.49 | 91.4 | 6.83 | 1.2 | 100 | 12.6 | 4.5 | 94.4 |
| 11^b | <i>N</i> -(1-Hexyl) | 18.2 | 3.9 | 87.3 | 10.7 | 0.62 | 98.6 | 16.6 | 4.4 | 77.9 |
| 12 | <i>N</i> -(1-Heptyl) | 46.2 | 13.9 | 81.7 | 19.0 | 1.2 | 97.9 | 28.8 | 2.8 | 69.6 |
| 13 | <i>N</i> -(1-Octyl) | 135 | 16.7 | 80.2 | 37.4 | 6.0 | 75.2 | 36.2 | 2.7 | 68.4 |
| 14 | <i>N</i> -(1-Nonyl) | 333 | 128 | 79.5 | 88.2 | 5.5 | 85.8 | 68.2 | 4.7 | 68.6 |
| 15 | <i>N</i> -(1-Decyl) | 92.8 | ^a | 83.6 | 45.0 | ^a | 92.5 | 1393 | ^a | 67.4 |
| 16 | <i>N</i> -(1-Undecyl) | 168 | ^a | 86.4 | 25.5 | ^a | 83.8 | 278 | ^a | 90.3 |
| 17 | <i>N</i> -(1-Dodecyl) | 109 | ^a | 82.6 | 53.7 | ^a | 95.6 | 238 | ^a | 56.5 |
| 18 | <i>N</i> -(1-Tridecyl) | 492 | ^a | 79.3 | 172 | ^a | 97.6 | 495 | ^a | 80.5 |
| 19 | Geranylamine | 48.1 | ^a | 84.2 | 20.1 | ^a | 95.7 | 40.5 | ^a | 89.0 |
| 20 | <i>N</i> -(1,3-Dimethylpentyl) | 9.6 | ^a | 91.4 | 2.3 | ^a | 96.3 | 13.7 | ^a | 89.9 |
| 21 | <i>N</i> -(1,4-Dimethylpentyl) | 3.37 | ^a | 76.6 | 2.81 | ^a | 96.2 | 28.6 | ^a | 94.1 |
| 22 | <i>N</i> -(1-Methylhexyl) | 10.7 | ^a | 98.2 | 2.60 | ^a | 96.5 | 1.84 | ^a | 89.0 |
| 23 | <i>N</i> -(1,5-Dimethylhexyl) | 8.97 | ^a | 89.6 | 3.57 | ^a | 95.1 | 5.76 | ^a | 87.7 |
| 24 | <i>N</i> -(1-Ethylhexyl) | 19.6 | ^a | 89.5 | 8.6 | ^a | 95.7 | 25.8 | ^a | 85.1 |
| 25 | <i>N</i> -(1-Methylheptyl) | 26.2 | ^a | 83.9 | 10.8 | ^a | 91.3 | 5.8 | ^a | 53.7 |
| 26 | <i>N</i> -[1-(1,1-Dimethylheptyl)] | 181 | 5.8 | 83.2 | 21.6 | 3.3 | 76.4 | 10.4 | 3.3 | 72.2 |
| 27 | <i>N</i> -(1-Methyldecyl) | 27.1 | ^a | 83.7 | 9.7 | ^a | 97.3 | 22.3 | ^a | 82.4 |

^a $n = 1$, compound obtained from parallel synthesis and assay concentration was grossly estimated.

^b Some results for this compound have been published previously (see Ref. 28).

2.2. Human CB1 receptor affinity

In hCB₁-transfected cells, affinity modestly increased from C4 to C5 side chain. As the side chain was increased beyond C5, affinity tended to decrease up to C9, where a slight increase in affinity was noted up to C11. Beyond this length, further extension led to decreased affinity. As was seen in rat brain, the branched alkyl amides showed higher affinity within the pentyl and hexyl analogs than that seen with the heptyl or decyl branched side chains. Examination of the alkyl amide analogs using transfected cell lines expressing the hCB₁ receptor showed an even greater discrepancy in the ability of these compounds to displace [³H]**3** as compared to either [³H]**2** or [³H]**5** (Table 2, Fig. 3). It is interesting to note that there is a structural trend by which systematic increases in the alkyl side chain length past C6 leads to an incremental decrease in affinity and percentage maximum displacement for [³H]**5**, a more pronounced loss of affinity and percentage maximum displacement with [³H]**2**, and a profound loss of affinity and displacing ability with [³H]**3**. The difference between the rat brain membrane preparation and the hCB₁ receptor transfects is quite remarkable when one considers that these two CB1 receptors possess approximately 99% homology in their sequences.

It was possible that the augmentation in these compounds' binding selectivity in hCB₁ transfects could be a result of the nature of transfected cell lines and not due to the differences in receptor sequence and structure. However, when these compounds were tested in human brain membrane preparations (cerebellum and cortex),

similar results were obtained (Fig. 4). Thus, all evidence obtained to date supports the conclusion that these long-chain alkyl amides are unique from all other classes of cannabinoid receptor ligands with regard to their ability to displace the various radioligands tested. The data also illustrate that despite a very high degree of sequence homology, the alkyl amides beyond C6 interact at rat and hCB₁ receptors quite differently.

2.3. Human CB2 receptor affinity

Those compounds that were obtained by conventional synthesis were further tested for their affinity at the CB2 receptor (Table 3). In most instances, these compounds were unable to completely displace [³H]**2** from the CB2 receptor at the highest concentration tested, indicating that the relative selectivity of the analogs for CB1 versus CB2 receptors was relatively unaffected by structural modifications at this substituent position. Indeed, the absence of CB2-selective ligands in our series of analogs is consistent with the observation that the CB2-selective antagonist **6**, when compared to **5**, has structural modifications in addition to the change at the aminopiperidine moiety that was explored in these studies.

2.4. Cannabinoid receptor-mediated alteration in GTP- γ -[³⁵S] binding

In addition to assessing CB1 and CB2 receptor affinities, several compounds were screened in a GTP- γ -[³⁵S] assay for characterization of the compounds as agonists, partial agonists, antagonists, or inverse agonists. The results

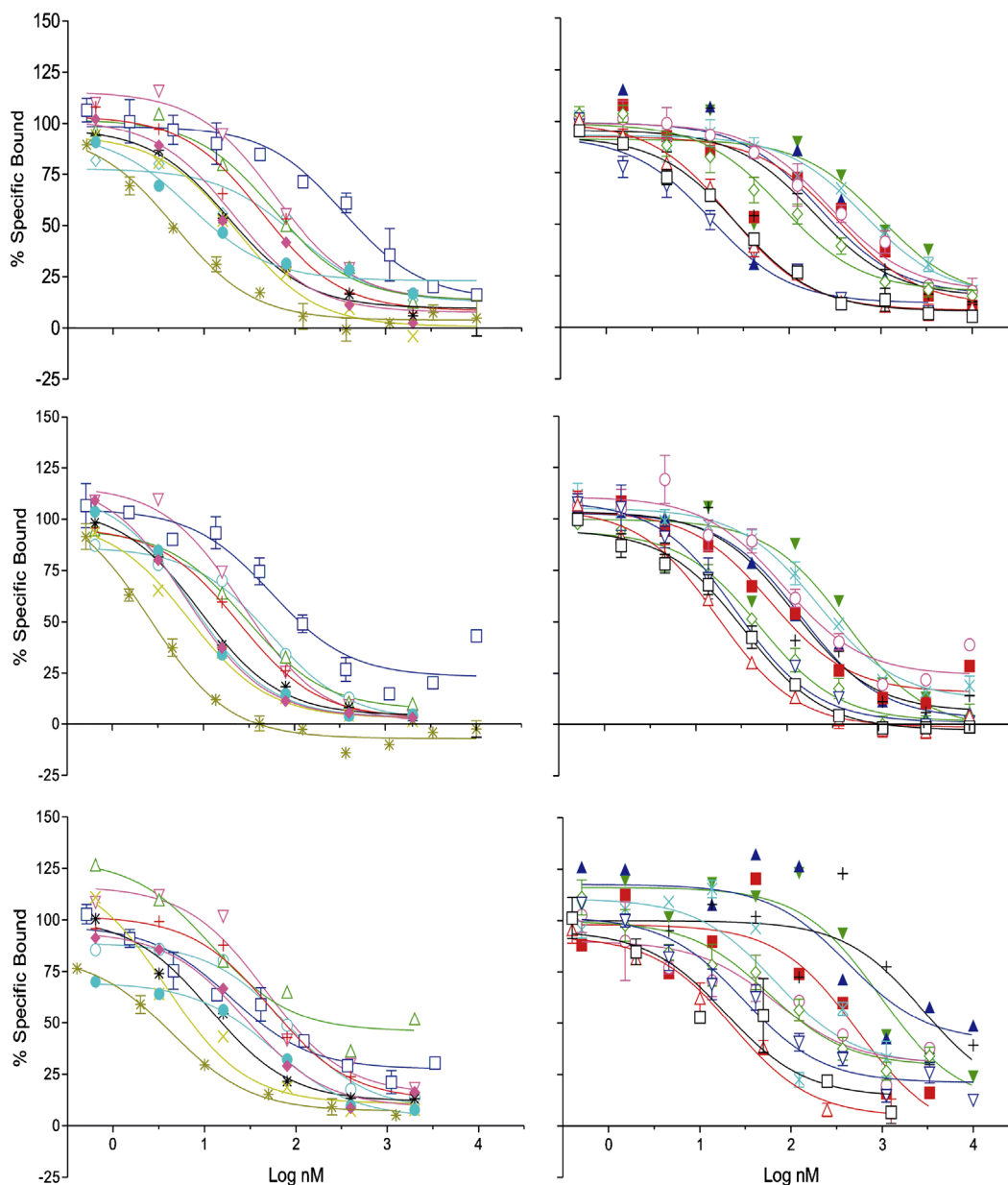


Figure 2. Displacement curves for SR141716A analogs in rat brain membrane against [^3H]CP55940 (top), [^3H]SR141716A (middle) and [^3H]WIN55212 (bottom) for (*) *N*-cyclohexyl, (◆) *N*-(1, 3-dimethylpentyl), (●) *N*-(1, 4-dimethylpentyl), (×) *N*-(1-methylhexyl), (✱) *N*-(1,5-dimethylhexyl), (+) *N*-(2-ethylhexyl), (□) *N*-(1,1-dimethylheptyl), (△) *N*-(1-methylheptyl), (▽) *N*-(1-methyldecyl) (left panel); and (○) 1-geranyl, (□) *N*-butyl, (△) *N*-pentyl, (▽) *N*-hexyl, (◇) *N*-heptyl, (○) *N*-octyl, (×) *N*-nonyl, (+) *N*-decyl, (■) *N*-undecyl, (▲) *N*-dodecyl, and (▼) *N*-tridecyl (right panel).

of GTP- γ -[^{35}S] studies (Table 4) demonstrate that, in all instances, these compounds act like inverse agonists.

When some of the alkyl amide compounds with the highest affinity for the CB1 receptor were characterized in an isolated mouse vas deferens, the results obtained (Table 4) support the conclusion that some of the alkyl amide analogs interact with the CB1 receptor in a unique manner. Specifically, one can see from the data in this table for the alkyl amides that as the chain length was increased from the butyl analog to the heptyl analog, the dextral shift in the dose–response curve of **3** was reduced. Indeed, in one experiment, the heptyl analog (**12**) failed to produce an effect on the dose–response curve, despite this compound having good affinity

(46.2 nM vs. [^3H]**2** in rat brain), and producing a robust inverse agonist effect in the absence of any application of **3**. Thus, the data suggest that this compound can interact at the receptor (displace [^3H]**2** and [^3H]**5**) and produce inverse agonist effects, but not readily compete for the WIN55212-2 (**3**) binding site, and thereby fail to produce a dextral shift in the dose–response curve until extremely high concentrations are used. This lends pharmacological significance to the aforementioned ‘WIN-sparing’ displacement curves (Figs. 2 and 3) obtained with the alkyl amide analogs. With extremely high concentrations of **12** (>3 μM), the dose–response curves for both **2** and **3** were shifted, albeit to a much lesser extent than that achieved with the prototype antagonist, **5**.

Table 2. Amide analogs at the 3-position: displacement of various radioligands in human CB1 receptor-transfected cells

| Compound | Substituted group | $[^3\text{H}]\mathbf{2}$ | | | $[^3\text{H}]\mathbf{5}$ | | | $[^3\text{H}]\mathbf{3}$ | | |
|-----------------------|------------------------------------|--------------------------|--------------|--------------------------|--------------------------|--------------|--------------------------|--------------------------|--------------|--------------------------|
| | | K_i (nM) | SEM | Maximum displacement (%) | K_i (nM) | SEM | Maximum displacement (%) | K_i (nM) | SEM | Maximum displacement (%) |
| 5 (SR141716) | | 3.92 | ^a | 79.5 | 2.43 | ^a | 85.7 | 4.67 | ^a | 77.9 |
| 8^c | <i>N</i> -(1-Cyclohexyl) | 7.06 | 0.76 | 92.3 | 1.02 | 0.22 | 99.9 | 5.36 | 0.24 | 96.8 |
| 9^c | <i>N</i> -(1-Butyl) | 28.0 | 1.3 | 90.2 | 4.79 | 0.89 | 97.4 | 29.8 | 15.6 | 93.2 |
| 10^c | <i>N</i> -(1-Pentyl) | 14.6 | 3.6 | 87.1 | 6.35 | 2.4 | 89.9 | 18.7 | 5.9 | 89.9 |
| 11^c | <i>N</i> -(1-Hexyl) | 124 | 27.4 | 85.6 | 23.5 | 16.5 | 75.4 | 85.4 | 18.6 | 52.7 |
| 12 | <i>N</i> -(1-Heptyl) | 291 | 69.7 | 85.3 | 9.3 | 1.1 | 67.9 | 393 | 154 | 53.4 |
| 13 | <i>N</i> -(1-Octyl) | 288 | 48.0 | 70.6 | 44.7 | 18.6 | 67.8 | ND ^b | 36.9 | 35.2 |
| 14 | <i>N</i> -(1-Nonyl) | 307 | 40.7 | 68.8 | 56.5 | 25.7 | 86.9 | ND ^b | 2826 | 28.3 |
| 15 | <i>N</i> -(1-Decyl) | 184 | ^a | 94.5 | 24.6 | ^a | 95.4 | ND ^b | ^a | 12.4 |
| 16 | <i>N</i> -(1-Undecyl) | 57.7 | ^a | 66.3 | 21.0 | ^a | 90.4 | 166 | ^a | 74.6 |
| 17 | <i>N</i> -(1-Dodecyl) | 176 | ^a | 79.5 | 43.5 | ^a | 89.8 | ND ^b | ^a | 31.4 |
| 18 | <i>N</i> -(1-Tridecyl) | 220 | ^a | 62.6 | 101 | ^a | 87.3 | 128 | ^a | 68.1 |
| 19 | Geranylamine | 26.8 | ^a | 84.2 | 6.80 | ^a | 95.7 | 211 | ^a | 78.3 |
| 20 | <i>N</i> -(1,3-Dimethylpentyl) | 9.4 | ^a | 86.5 | 2.2 | ^a | 100 | 23.9 | ^a | 78.7 |
| 21 | <i>N</i> -(1,4-Dimethylpentyl) | 13.2 | ^a | 76.8 | 5.48 | ^a | 93.6 | 33.2 | ^a | 91.5 |
| 22 | <i>N</i> -(1-Methylhexyl) | 11.9 | ^a | 80.7 | 2.02 | ^a | 95.6 | 54.6 | ^a | 100 |
| 23 | <i>N</i> -(1,5-Dimethylhexyl) | 7.39 | ^a | 82.5 | 2.10 | ^a | 93.7 | 64.2 | ^a | 67.9 |
| 24 | <i>N</i> -[1-(2-Ethyl)hexyl] | 9.6 | ^a | 91.4 | 3.8 | ^a | 95.9 | 78.6 | ^a | 100 |
| 25 | <i>N</i> -(1-Methylheptyl) | 26.3 | ^a | 79.5 | 2.8 | ^a | 91.5 | ND ^c | ^a | 0.0 |
| 26 | <i>N</i> -[1-(1,1-Dimethylheptyl)] | 32.7 | 10.4 | 91.1 | 5.0 | 0.51 | 99.9 | 14.4 | 1.0 | 86.5 |
| 27 | <i>N</i> -(1-Methyldeacyl) | 41.1 | ^a | 77.7 | 7.0 | ^a | 90.0 | 22.2 | ^a | 76.1 |

^a $n = 1$, compound obtained from parallel synthesis and assay concentration was grossly estimated.

^b The K_i value could not be determined since <50% displacement of the radiolabel occurred.

^c Some results for this compound have been published previously (see Ref. 28).

Since compound **12** appeared to be unable to fully displace $[^3\text{H}]\mathbf{3}$, it was further tested in GTP- γ - $[^{35}\text{S}]$ experiments to compare the ability of **5** and **12** to shift the dose–response curve of CP55940 (**2**) or WIN55212-2 (**3**). The results of these assays are provided in Table 5. When the model is constrained to one where the Schild slope is 1, the pA_2 values are equal to the pK_b of the antagonist. In this instance, the pK_b values are consistent with the K_i values. For example, the pK_i of **5** in rat brain is 8.21 against $[^3\text{H}]\mathbf{2}$ and 8.71 against $[^3\text{H}]\mathbf{3}$, and in hCB₁-transfected cells, it is 8.41 against $[^3\text{H}]\mathbf{2}$ and 8.33 against $[^3\text{H}]\mathbf{3}$. These K_i values are in reasonably close correspondence with the K_b values (K_b calculated with a Schild slope constrained to 1) in rat brain of 9.28 against $[^3\text{H}]\mathbf{2}$ and 9.49 against $[^3\text{H}]\mathbf{3}$, and 7.55 against $[^3\text{H}]\mathbf{2}$ and 7.79 against $[^3\text{H}]\mathbf{3}$ in hCB₁-transfected cells. Similarly, the pK_i of **12** in rat brain is 7.34 against $[^3\text{H}]\mathbf{2}$ and 7.54 against $[^3\text{H}]\mathbf{3}$, and in hCB₁-transfected cells, it is 6.54 against $[^3\text{H}]\mathbf{2}$ and 6.41 against $[^3\text{H}]\mathbf{3}$. Comparing these K_i values to the K_b values in rat brain of 9.00 against $[^3\text{H}]\mathbf{2}$ and 7.52 against $[^3\text{H}]\mathbf{3}$, and 7.24 against $[^3\text{H}]\mathbf{2}$ and 7.24 against $[^3\text{H}]\mathbf{3}$ in hCB₁-transfected cells. However, there does not appear to be a difference in the ability of **12** to antagonize the effects of **2** as compared to **3**, as might have been expected based on **12**'s selective binding displacement data.

3. Discussion

The nature of the substituent at the 3-position has a marked effect on receptor binding affinity. Previous research has shown that increasing the length and

branching of alkyl amide chains up to five carbons in length results in modest increases in affinity at rat brain CB1 receptor preparations, a trend that is also apparent in hydroxy alkyl amide and hydrazide analogs. After the pentyl analog, additional chain lengthening of alkyl amides resulted in a further decrease in affinity. However, as the carbon chain extended beyond C5 or C6, affinity tends to decrease, and the ability to fully displace $[^3\text{H}]\mathbf{3}$ decreases in a more pronounced fashion than observed with $[^3\text{H}]\mathbf{2}$ and $[^3\text{H}]\mathbf{5}$. It is important to note that the compounds with side chains extending beyond C9 (nonyl), and the majority of the branched alkyl amides, were synthesized using parallel synthesis techniques. While we used LC/UV/MS methods to ensure that the yields were relatively consistent from one compound to another, the concentrations of these compounds were estimated based on approximately 50% recovery, as suggested by the HPLC/UV response. Thus, substantive conclusions regarding relative affinities within these compounds should be avoided, but observations regarding the percentage maximum displacement in binding displacement studies are supportable, as long as the sigmoidal curves show no further decrease with increasing concentrations. Furthermore, characterization in mouse vas deferens studies with **3** also indicated that these compounds were pharmacologically unique, and this encouraged us to extend our observations into other CB1 receptor preparations. In CHO cells transfected with hCB₁ and in human postmortem tissue, this unique selectivity was more pronounced, despite the high degree of homology between the two receptors (hCB₁ and rCB₁). This selectivity in displacement has not previously been reported for a cannabinoid compound in

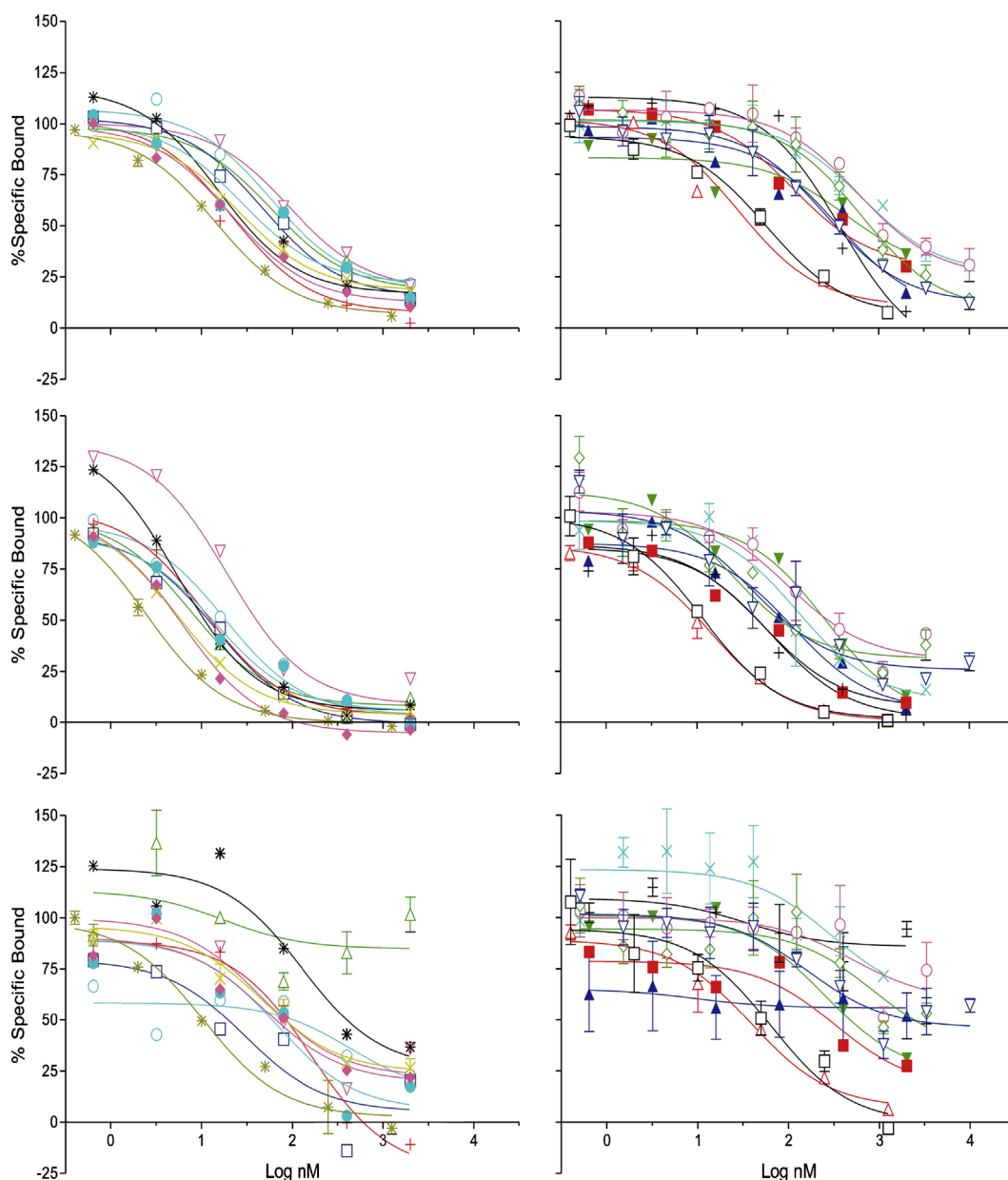


Figure 3. Displacement curves for SR141716A analogs in hCB1-transfected cells against [3 H]CP55940 (top), [3 H]SR141716A (middle), and [3 H]WIN55212 (bottom) for (*) *N*-cyclohexyl, (◆) *N*-(1, 3-dimethylpentyl), (●) *N*-(1, 4-dimethylpentyl), (×) *N*-(1-methylhexyl), (✱) *N*-(1,5-dimethylhexyl), (+) *N*-(2-ethylhexyl), (□) *N*-(1,1-dimethylheptyl), (△) *N*-(1-methylheptyl), (▽) *N*-(1-methyldecyl) (left panel); and (○) 1-geranyl, (□) *N*-butyl, (△) *N*-pentyl, (▽) *N*-hexyl, (◇) *N*-heptyl, (○) *N*-octyl, (×) *N*-nonyl, (+) *N*-decyl, (■) *N*-undecyl, (▲) *N*-dodecyl, and (▼) *N*-tridecyl (right panel).

wildtype CB1 receptors. That is, compounds within structural classes that bind to the CB1 receptor (i.e., the aminoalkylindole agonists such as **3**, the bicyclic cannabinoids such as **2**, and the pyrazole inverse agonists such as **5**) had always been shown to displace each other in a competitive fashion.

Evidence of unique binding domains for structurally divergent cannabinoid agonists has previously been provided only by receptor mutagenesis studies. For example, Song and Bonner used site-directed mutagenesis of the amino acids at position 5.46 of CB1 and CB2; a Phe to Val mutation at the position 5.46 in CB2 (CB2F5.46V), and a corresponding Val to Phe mutation at the position 5.46 in CB1 (CB1V5.46F).³¹ The mutant

receptors were transfected into human embryonic kidney (HEK293) cells and used for ligand binding and cAMP accumulation studies. The affinity of **3** for the CB2F5.46V mutation was decreased by 14-fold, whereas the CB(1)V5.46F mutation increased the affinity of **3** for CB₁ by 12-fold. However, these mutations did not change the affinity of HU-210, **2**, or **4**. Similarly, Lys192 of the third transmembrane domain of the CB1 receptor has been mutated to either Arg (K192R), Gln (K192Q), or Glu (K192E) receptors and expressed in Chinese hamster ovary cells.³² In this instance, only the Lys to Arg mutation allowed retention of binding affinity to **2**, whereas **3** bound to all the mutant receptors in the same range as it bound to the wildtype. More recently, Picone et al. reported at the 2002

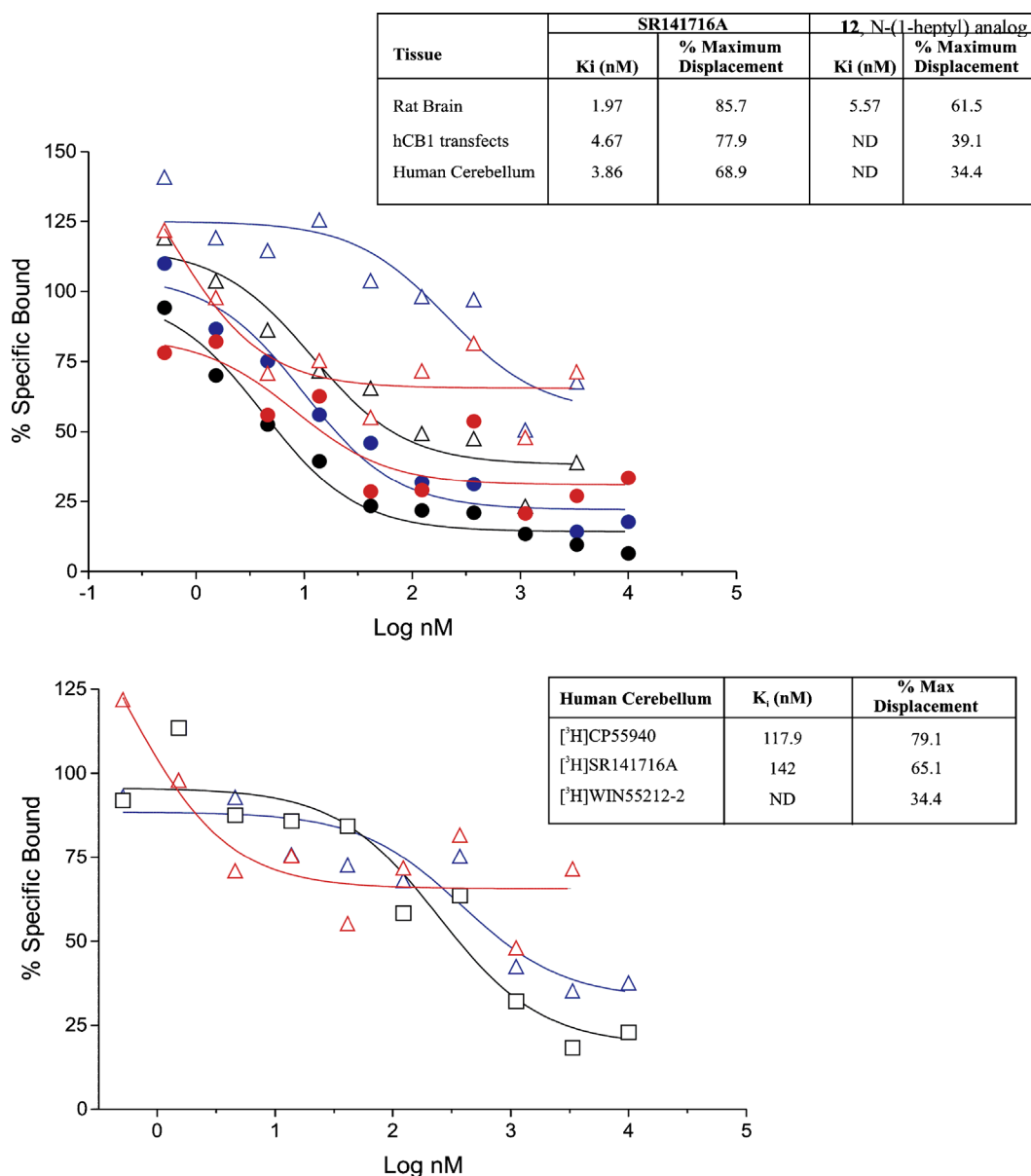


Figure 4. Presented in the top panel are [³H]WIN55212-2 competition curves for SR141716A (solid symbols) and the *N*-(1-heptyl)-analog of SR141716A (**12**, open symbols) as determined in rat brain (black symbols), human CB receptor-transfected cells (blue symbols), and human cerebellar membrane preparations (red symbols). In the bottom panel, displacement curves in human cerebellum for the *N*-(1-heptyl)-analog are shown as determined with [³H]CP55940 (□), [³H]SR141716A (Δ), and [³H]WIN55212-2 (Δ). In the inserts, the *K_i* and % maximum displacement are provided as determined for each curve. In those instances where <50% displacement occurred with a particular ligand, the *K_i* was not determined (ND).

meeting of the International Cannabinoid Research Society that mutation of the CB1 receptor amino acid residue C6.47(355) to S, A, I, and K impacts the receptor binding affinity of [³H]CP55940, while leaving the binding of [³H]WIN55212-2 unaffected.³³ All of these studies support the hypothesis that WIN55212-2 binds differently to the CB1 receptor than CP55940 and possibly other agonists and antagonists, which is consistent with the displacement curves we have described for the long-chain alkyl amides.

The heterologous displacement curves obtained with the long-chain alkyl amides suggest that these ‘WIN-sparing’ compounds also appear to be unique in their

receptor interactions as compared to SR141716. Indeed, it is possible that these compounds have other pharmacological properties that are unique from SR141716 or other antagonists that displace all other cannabinoid ligands with equal capacity. The selective displacement of the agonists [³H]**2** and [³H]**3** seen with **12** as compared to **5** did not appear to translate into observable differences in antagonism of these agonists when tested in the GTP-γ-[³⁵S] assay. However, in the mouse vas deferens experiments, concentrations of **12** that possessed inverse agonist activity when tested alone, appeared less able to block the effects of either agonist when compared to **5**. This discrepancy in pharmacological antagonism/inverse agonist activity may be due to several factors.

Table 3. Amide analogs at the 3-position: displacement of [³H]CP55940 in human CB2 receptor-transfected cells

| Compound | Substituted group | [³ H]2 | | | |
|-----------------------|------------------------------------|---------------------|--------------|--------------------------|---------------|
| | | K _i (nM) | SEM | Maximum displacement (%) | Ratio CB1/CB2 |
| 5 (SR141716) | | 313 | ^a | | 79.8 |
| 6 (SR144528) | | 4.92 | 0.39 | 88.4 | ND |
| 8^b | <i>N</i> -(1-Cyclohexyl) | 228 | 1.5 | 84.5 | 32.3 |
| 9^b | <i>N</i> -(1-Butyl) | 1598 | 425 | 75.6 | 57.1 |
| 10^b | <i>N</i> -(1-Pentyl) | 1110 | 241 | 75.9 | 76.0 |
| 11^b | <i>N</i> -(1-Hexyl) | 6873 | ^a | 66.9 | 55.4 |
| 12 | <i>N</i> -(1-Heptyl) | 4027 | 174 | 47.8 | 13.8 |
| 13 | <i>N</i> -(1-Octyl) | 98,366 | 92,734 | 45.3 | 342 |
| 14 | <i>N</i> -(1-Nonyl) | 22,878 | 17,622 | 53.8 | 74.5 |
| 26 | <i>N</i> -[1-(1,1-Dimethylheptyl)] | 16,555 | 3445 | 52.8 | 506 |

^a *n* = 1.^b Some results for this compound have been published previously (see Ref. 28).**Table 4.** Amide analogs at the 3-position: inverse agonist/antagonist activity

| Compound | Substituted group | GTP-γ-[³⁵ S] in whole rat brain | | | Mouse vas deferens tissue assay | | | | | |
|---------------------|--------------------------|---|---------|------------------|---------------------------------|--------------------|---------------------|------------------|-------------------------|--|
| | | EC ₅₀ (nM) | SEM | E _{max} | Agonist used | [nM] | K _b (nM) | Dextral shift | % Inverse effect | |
| 5 (SR141716) | | 56,305 | 14,330 | -37.8 | 3 | 31.6 | 0.4 | 81.4 | 65.2 | |
| 6 (SR144528) | | 8136 | 258 | -27.7 | | | | | | |
| 8 | <i>N</i> -(1-Cyclohexyl) | 26,030 | — | -22.1 | 3 | 31.6 | 1.2 | 26.7 | 55.5 | |
| 9 | <i>N</i> -(1-Butyl) | 8536 | 3134 | -38.5 | 3 | 316.2 | 21.2 | 15.9 | NS ^c (28.2) | |
| 10 | <i>N</i> -(1-Pentyl) | 5270 | 1656 | -7.4 | 3 | 316.2 | 31.7 | 11.0 | 86.6 | |
| 11 | <i>N</i> -(1-Hexyl) | 29,375 | 16,135 | -13.0 | 3 | 31.6 | 15.4 | 3.1 | NS (30.1) | |
| 12 | <i>N</i> -(1-Heptyl) | 212,950 | 3950 | -20.0 | 3 | 316.2 | NS | NS | 50.6 | |
| | | | | | 3 | 316.2 ^b | 83.9 ^b | 4.8 ^b | NS (37.8 ^b) | |
| | | | | | 3 | 3162 | 100.4 | 32.5 | 49.3 | |
| | | | | | 2 | 3162 | 157.1 | 21.1 | NS (15.0) | |
| 13 | <i>N</i> -(1-Octyl) | 676,800 ^a | 187,400 | -21.3 | | | | | | |
| 14 | <i>N</i> -(1-Nonyl) | 293,500 | 60,400 | -20.1 | | | | | | |

^a Value is above highest concentration on displacement curve.^b Due to unexpected result, compound was assayed again and both replicates are shown.^c NS = not significant.**Table 5.** Schild analysis of the antagonism of CP55940 and WIN55212-2 by **5** and **12** in rat brain and hCB₁-transfected CHO cells

| Agonist | SR141716A (5) | | | | 12 | | | |
|-------------------------------|---------------------------------|----------------------|---------------------------------|----------------------|---------------------------------|----------------------|---------------------------------|----------------------|
| | Rat brain | | hCB ₁ cells | | Rat brain | | hCB ₁ cells | |
| | pA ₂ /K _b | Slope/R ² |
| Schild slope constrained to 1 | | | | | | | | |
| CP55940 | 9.28 | 1/0.01 | 7.55 | 1/-0.09 | 9.0 | 1/0.26 | 7.24 | 1/0.12 |
| WIN55212 | 9.49 | 1/0.61 | 7.79 | 1/0.20 | 7.52 | 1/0.41 | 7.24 | 1/0.25 |
| Schild slope not constrained | | | | | | | | |
| CP55940 | 8.55 | 1.87/0.13 | 7.07 | 7.63/-0.08 | 10.4 | 0.55/0.33 | 22.61 | 0.05/0.21 |
| WIN55212 | 9.91 | 0.81/0.62 | 7.10 | 6.81/-0.19 | 13.88 | 0.12/0.55 | 7.54 | 0.55/0.25 |

The data derived using the statistically better model (determined using global nonlinear regression and an *F*-test, see Methods) is shown in bold.

For example, it is possible that **2** and **3** and **5** and **12** differ in their influence on GPCR activation beyond their effects on the relative proportion of the receptor active state. It has been shown that chemically distinct classes of cannabinoid agonists promote differential CB₁ receptor-Gi protein interactions.³⁴ It is also likely that antagonists are able to induce differing populations of microconformations of the CB₁ receptor, which could have an effect on their G-protein uncoupling and specificity. However, the significance in the binding affinity and signaling differences between **5** and **12** needs to be

further characterized in *in vitro* and *in vivo* assays of cannabinoid activity.

It is intriguing to speculate that there may be other cannabinoid ligands that are spared from displacement with these unique SR141716 analogs. For example, it remains to be determined whether endocannabinoids are displaced by 'WIN-sparing' SR141716 analogs. If they are not, it is possible that the endocannabinoid system could be left unaltered, while some exogenous cannabinoid compounds could be antagonized. However, it is

also possible that the unique binding of the alkyl compounds imparts unique pharmacological properties in the absence of a competitive agonist or antagonist. These possibilities will therefore be the subject of future exploration in our laboratory.

4. Experimental

The synthesis of the target compounds **8–11** was described previously,²⁸ and compounds **12**, **13**, and **26** were synthesized in a manner similar to a previously published synthesis of **5**²⁸ by condensation of the respective amines with the pyrazole acid chloride **7**, as shown in Scheme 1.

Dimethylheptyl amine was prepared by the addition of ethyl 2,2-dimethyloctanoate to sodium amide in tetrahydrofuran (THF),²⁹ followed by Hofmann rearrangement using the commercially available reagent [*I,I*-bis(trifluoroacetoxy)iodo]benzene.³⁰ The synthesis of **26** was then carried out as above (Scheme 1). The products were characterized by ¹H nuclear magnetic resonance (NMR), high-resolution electron impact (EI) mass spectroscopy, and HPLC.

The synthesis of the target compounds **15–25** and **27** was carried out by similar methods as previously published,²⁸ performed in parallel using an Argonaut Quest 210.

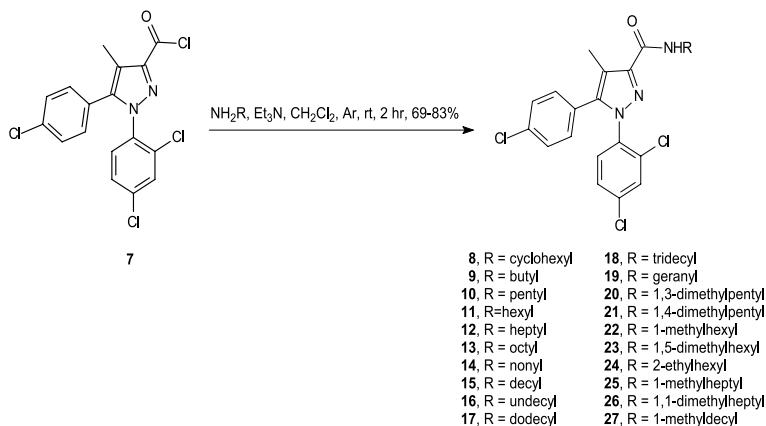
4.1. General methods

Reactions were conducted under N₂ or Ar atmospheres using oven-dried glassware. Parallel syntheses were performed with an Argonaut Technologies Quest 210 Parallel Synthesizer. All solvents and chemicals used were reagent grade. CH₂Cl₂ was passed through basic alumina and stored over 4 Å molecular sieves under Ar. Et₃N was distilled from CaH₂ and stored over NaOH pellets under Ar. Unless otherwise mentioned, reagents were obtained from commercial sources and used without further purification. Medium-pressure column chromatography was carried out on a Merck LoBar prepacked silica gel column (240 mm, Si-60, 40–63 μm). Purity and characterization of compounds were established by a

combination of HPLC, GC–MS, high-resolution mass spectra (HRMS), LC/MS, and NMR analytical techniques described below. Compounds were shown to be homogeneous by HPLC, employing two diverse solvent mixtures on a Waters dual pump chromatography operating at 2.0 mL/min with a model 484 tunable absorbance detector, Waters Nova-Pak reversed phase C-18 (4 μm) RCM 8 mm × 100 mm column, and UV detection at 280 nm; eluants utilized were either CH₃CN–H₂O or CH₃OH–H₂O mixtures as indicated in each experimental procedure. GC–MS was measured on a Hewlett–Packard 6890 GC System with a model 5973 Mass Selective Detector using EI ionization. LC/MS spectra were obtained using an API3000 LC/MS-MS system using atmospheric pressure chemical ionization (APCI). HRMS were determined on a VG-70S Mass Spectrometer (Micromass, Beverly, MA) and were performed by the mass spectrometry laboratory at the University of South Carolina. ¹H NMR spectra were recorded on a Bruker Avance DPX-300 (300 MHz) spectrometer and were determined in MeOH-*d*₄ with TMS (0.00 ppm) or MeOH (3.30 ppm) as the internal reference unless otherwise noted.

4.2. *N*-(1-Heptyl)-5-(4-chlorophenyl)-1-(2,4-dichlorophenyl)-4-methyl-1*H*-pyrazole-3-carboxamide (**12**)

1-Heptylamine (172.5 mg, 222.0 μL, 1.50 mmol), triethylamine (420 μL, 3.00 mmol), and CH₂Cl₂ (7 mL) were cooled to 0 °C under argon and treated dropwise over 5 min with a solution of **7**²⁸ (299.1 mg, 0.75 mmol) in CH₂Cl₂ (8 mL). The solution was allowed to warm slowly to 25 °C under Ar and stirred for an additional 2 h. The reaction was quenched by the addition of 10 mL H₂O and partitioned. The organic layer was washed with 2 × 20 mL of 1 N HCl. The combined aqueous layers were backextracted with CH₂Cl₂, and the combined CH₂Cl₂ layers were washed with saturated aqueous NaHCO₃. The aqueous layer was backextracted with CH₂Cl₂, and the combined CH₂Cl₂ layers were dried over Na₂SO₄. The CH₂Cl₂ was evaporated in vacuo, yielding a yellow oil. Medium-pressure chromatography (1:7, EtOAc–hexanes) yielded the product as a yellow oil (286 mg, 80% yield). ¹H NMR: δ 7.59 (d, *J* = 2.2 Hz, 1H, Ar 3-H), 7.55 (d, *J* = 8.5 Hz, 1H, Ar 6-H), 7.46 (dd, *J* = 2.2, 8.5 Hz, 1H, Ar 5-H), 7.39 (d, *J* = 8.5 Hz,



Scheme 1.

2H, Ar' 3,5-H), 7.21 (d, $J = 8.5$ Hz, 2H, Ar' 2,6-H), 3.37 (t, $J = 7.1$ Hz, 2H, N-CH₂-(CH₂)₅-CH₃), 2.32 (s, 3H, CH₃), 1.62 (m, 2H, N-CH₂-CH₂-(CH₂)₄-CH₃), 1.36 (m, 8H, N-CH₂-CH₂-(CH₂)₄-CH₃), 0.91 (t, $J = 6.8$ Hz, 3H, N-(CH₂)₆-CH₃). HPLC: 90% CH₃CN-H₂O, t_R 6.5 min (100%); 85% CH₃OH-H₂O, R_t 12.2 min (100%). HREIMS m/z 477.1141 (calcd for C₂₅H₂₈³⁵Cl₃N₃O, 477.1141).

4.3. *N*-(1-Octyl)-5-(4-chlorophenyl)-1-(2,4-dichlorophenyl)-4-methyl-1*H*-pyrazole-3-carboxamide (13)

Compound **7** was obtained from **4** and 1-octylamine according to the procedure described for **6** and was isolated as a yellow oil (175 mg, 90% yield). ¹H NMR: δ 7.54 (d, $J = 2.2$ Hz, 1H, Ar 3-H), 7.50 (d, $J = 8.5$ Hz, 1H, Ar 6-H), 7.42 (dd, $J = 2.2, 8.5$ Hz, 1H, Ar 5-H), 7.35 (d, $J = 8.5$ Hz, 2H, Ar' 3,5-H), 7.18 (d, $J = 8.5$ Hz, 2H, Ar' 2,6-H), 3.34 (t, $J = 7.2$ Hz, 2H, N-CH₂-(CH₂)₆-CH₃), 2.30 (s, 3H, CH₃), 1.59 (m, 2H, N-CH₂-CH₂-(CH₂)₅-CH₃), 1.28 (m, 10H, N-CH₂-CH₂-(CH₂)₅-CH₃), 0.88 (t, $J = 7.0$ Hz, 3H, N-(CH₂)₇-CH₃). HPLC: 90% CH₃CN-H₂O, t_R 16.6 min (99%); 85% CH₃OH-H₂O, R_t 16.3 min (100%). HREIMS m/z 491.1277 (calcd for C₂₅H₂₈³⁵Cl₃N₃O, 491.1298).

4.4. *N*-(1-Nonyl)-5-(4-chlorophenyl)-1-(2,4-dichlorophenyl)-4-methyl-1*H*-pyrazole-3-carboxamide (14)

Compound **8** was obtained from **4** and 1-nonylamine according to the procedure described for **7** and was isolated as a yellow oil (211 mg, 83% yield). ¹H NMR: δ 7.50 (d, $J = 2.2$ Hz, 1H, Ar 3-H), 7.47 (d, $J = 8.5$ Hz, 1H, Ar 6-H), 7.39 (dd, $J = 2.2, 8.5$ Hz, 1H, Ar 5-H), 7.31 (d, $J = 8.5$ Hz, 2H, Ar' 3,5-H), 7.14 (d, $J = 8.5$ Hz, 2H, Ar' 2,6-H), 3.30 (t, $J = 7.1$ Hz, 2H, N-CH₂-(CH₂)₇-CH₃), 2.26 (s, 3H, CH₃), 1.54 (m, 2H, N-CH₂-CH₂-(CH₂)₆-CH₃), 1.24 (m, 12H, N-CH₂-CH₂-(CH₂)₆-CH₃), 0.84 (t, $J = 6.8$ Hz, 3H, N-(CH₂)₈-CH₃). HPLC: 90% CH₃CN-H₂O, t_R 21.6 min (99%); 85% CH₃OH-H₂O, R_t 23.2 min (100%). HREIMS m/z 505.1463 (calcd for C₂₆H₃₀³⁵Cl₃N₃O, 505.1454).

4.5. Synthesis of 2,2-dimethyloctanamide²⁹

NaNH₂ (10.1 mmol) was treated with a solution of ethyl 2,2-dimethyloctanoate^{35,36} (10.1 mmol) in dry THF (35 mL) under N₂ and stirred at ambient temperature for 2 h. The reaction was quenched with saturated aqueous NH₄Cl. This was extracted with 2 × 20 mL CH₂Cl₂. The organic layer was washed with 2 × 20 mL saturated aqueous NH₄Cl, and the combined organic layers were dried over Na₂SO₄. The CH₂Cl₂ was evaporated in vacuo, yielding a beige powder (1.02 g, 59% yield). The product was carried forth to the next step without further purification.

4.6. Synthesis of 1,1-dimethylheptyl amine³⁰

[*I,I*-bis(trifluoroacetoxy)iodo]benzene (703 mg, 4.1 mmol) was dissolved in acetonitrile (6 mL) and glass-distilled water (6 mL) was added. To this solution, 2,2-dimethyloctanamide (1.94 g, 4.5 mmol) was added and

the solution was stirred in the dark at room temperature for 12 h. The reaction mixture was diluted with water (75 mL), concentrated HCl (8 mL) was added, and the mixture was extracted with ether (2 × 75 mL). The aqueous layer was concentrated at reduced pressure to yield the hydrochloride salt of 1,1-dimethylheptylamine as white, needle-like crystals (662 mg, 96% yield). mp 112.2–112.8 °C.

4.7. *N*-(1,1-Dimethylheptyl)-5-(4-chlorophenyl)-1-(2,4-dichlorophenyl)-4-methyl-1*H*-pyrazole-3-carboxamide (26)

The HCl salt of 1,1-dimethylheptyl amine (174.1 mg, 1.03 mmol), triethylamine (500 μ L, 3.59 mmol) and 95% EtOH (5 mL) were cooled to 0 °C under argon and treated dropwise over 5 min with a solution of **4** (203.6 mg, 0.51 mmol) in CH₂Cl₂ (5 mL). The solution was allowed to warm slowly to 25 °C under Ar and stirred for an additional 2 h. The reaction was quenched by addition of 10 mL H₂O. The organic layer was washed with 2 × 20 mL of 1 N HCl. The combined aqueous layers were backextracted with CH₂Cl₂, and the combined CH₂Cl₂ layers were washed with saturated aqueous NaHCO₃. The aqueous layer was backextracted with CH₂Cl₂, and the combined CH₂Cl₂ layers were dried over Na₂SO₄. The CH₂Cl₂ was evaporated in vacuo, yielding a dark yellow film. Flash chromatography (1:11, EtOAc-hexanes) yielded the product as a yellow oil (177.2 mg, 69% yield). ¹H NMR: δ 7.57 (d, $J = 2.1$ Hz, 1H, Ar 3-H), 7.52 (d, $J = 8.5$ Hz, 1H, Ar 6-H), 7.44 (dd, $J = 2.2, 8.5$ Hz, 1H, Ar 5-H), 7.36 (d, $J = 8.5$ Hz, 2H, Ar' 3,5-H), 7.18 (d, $J = 8.5$ Hz, 2H, Ar' 2,6-H), 2.28 (s, 3H, CH₃), 1.80 (br t, $J = 7.5$ Hz, 2H, N-C(CH₃)₂-CH₂-(CH₂)₄-CH₃), 1.40 (s, 6H, N-C(CH₃)₂-(CH₂)₅-CH₃), 1.31 (m, 8H, N-C(CH₃)₂-CH₂-(CH₂)₄-CH₃), 0.88 (t, $J = 6.0$ Hz, 3H, N-C(CH₃)₂-(CH₂)₅-CH₃). HPLC: 90% CH₃CN-H₂O, R_t 24.7 min (99%); 80% CH₃OH-H₂O, t_R 24.3 min (100%). HREIMS m/z 505.1465 (calcd for C₂₆H₃₀³⁵Cl₃N₃O, 505.1454).

4.8. Preparation of long-chain unbranched- and branched-alkyl amide analogs of (5): general procedure

To a mixture of the respective hydrazine or alkyl amine (0.09 mmol) and Et₃N (0.18 mmol) in anhydrous CH₂Cl₂ (4 mL) under nitrogen, **7** (0.05 mmol) was added, and the reaction mixture was agitated for 2 h at room temperature. The crude mixtures were washed with water, the layers were separated, and the organics were dried over Na₂SO₄. Filtration and solvent removal yielded the desired compounds which were characterized by ¹H NMR and/or LC/MS.

4.9. *N*-(1-Decyl)-5-(4-chlorophenyl)-1-(2,4-dichlorophenyl)-4-methyl-1*H*-pyrazole-3-carboxamide (15)

¹H NMR (CD₃OD): δ 7.56 (d, $J = 2.2$ Hz, 1H), 7.52 (d, $J = 8.5$ Hz, 1H), 7.44 (dd, $J = 2.2$ Hz, 8.5 Hz, 1H), 7.36 (d, $J = 8.5$ Hz, 2H), 7.19 (d, $J = 8.5$ Hz, 2H), 3.35 (t, $J = 7.1$ Hz), 2.30 (s, 3H), 1.60 (m, 2H), 1.28 (m, 14H), 0.89 (t, $J = 6.6$ Hz, 3H).

4.10. *N*-(1-Undecyl)-5-(4-chlorophenyl)-1-(2,4-dichlorophenyl)-4-methyl-1*H*-pyrazole-3-carboxamide (16)

¹H NMR (CD₃OD): δ 7.56 (d, *J* = 2.2 Hz, 1H), 7.52 (d, *J* = 8.5 Hz, 1H), 7.44 (dd, *J* = 2.2 Hz, 8.5 Hz, 1H), 7.36 (d, *J* = 8.5 Hz, 2H), 7.19 (d, *J* = 8.5 Hz, 2H), 3.35 (t, *J* = 7.1 Hz, 2H), 2.30 (s, 3H), 1.59 (m, 2H), 1.28 (m, 16H), 0.89 (t, *J* = 6.6 Hz, 3H).

4.11. *N*-(1-Dodecyl)-5-(4-chlorophenyl)-1-(2,4-dichlorophenyl)-4-methyl-1*H*-pyrazole-3-carboxamide (17)

¹H NMR (CD₃OD): δ 7.56 (d, *J* = 2.1 Hz, 1H), 7.52 (d, *J* = 8.5 Hz, 1H), 7.44 (dd, *J* = 2.1 Hz, 8.5 Hz, 1H), 7.36 (d, *J* = 8.4 Hz, 2H), 7.19 (d, *J* = 8.4 Hz, 2H), 3.52 (t, *J* = 7.1 Hz, 2H), 2.30 (s, 3H), 1.60 (m, 2H), 1.28 (m, 18H), 0.89 (t, *J* = 6.6 Hz, 3H).

4.12. *N*-(1-Tridecyl)-5-(4-chlorophenyl)-1-(2,4-dichlorophenyl)-4-methyl-1*H*-pyrazole-3-carboxamide (18)

¹H NMR (CD₃OD): δ 7.56 (d, *J* = 2.2 Hz, 1H), 7.52 (d, *J* = 8.5 Hz, 1H), 7.44 (dd, *J* = 2.2 Hz, 8.5 Hz, 1H), 7.36 (d, *J* = 8.5 Hz, 2H), 7.19 (d, *J* = 8.5 Hz, 2H), 3.35 (t, *J* = 7.1 Hz, 2H), 2.30 (s, 3H), 1.58 (m, 2H), 1.28 (m, 20H), 0.89 (t, *J* = 6.6 Hz, 3H).

4.13. *N*-(1-Geranyl)-5-(4-chlorophenyl)-1-(2,4-dichlorophenyl)-4-methyl-1*H*-pyrazole-3-carboxamide (19)

¹H NMR (CDCl₃): δ 7.42 (s, 1H), 7.28 (m, 4H), 7.01 (d, *J* = 8.5 Hz, 2H), 6.86 (t, *J* = 9.0 Hz, 1H), 5.28 (t, *J* = 8.3 Hz, 1H), 5.08 (t, *J* = 8.3 Hz, 1H), 4.03 (t, *J* = 8.2 Hz, 2H), 2.38 (s, 3H), 2.03 (m, 4H), 1.70 (s, 3H), 1.66 (s, 3H), 1.56 (s, 3H). LC/UV-MS analysis revealed a single UV peak at 11.68 min (~93% integrated area) with an intense ion (base peak) at *m/z* 538 (predicted mass of sodium adduct).

4.14. *N*-(1,3-Dimethylpentyl)-5-(4-chlorophenyl)-1-(2,4-dichlorophenyl)-4-methyl-1*H*-pyrazole-3-carboxamide (20)

¹H NMR (CDCl₃): δ 7.43 (s, 1H), 7.30 (m, 4H), 7.04 (d, *J* = 8.5 Hz, 2H), 6.73 (d, *J* = 8.0 Hz, 5H), 6.67 (d, *J* = 8.0 Hz, 5H), 4.27 (m, 1H), 2.38 (s, 3H), 1.47 (m, 3H), 1.20 (m, 5H), 0.89 (m, 6H). LC/UV-MS analysis revealed a single UV peak at 11.16 min (~97% integrated area) with an intense ion (base peak) at *m/z* 500 (predicted mass of sodium adduct).

4.15. *N*-(1,4-Dimethylpentyl)-5-(4-chlorophenyl)-1-(2,4-dichlorophenyl)-4-methyl-1*H*-pyrazole-3-carboxamide (21)

¹H NMR (CDCl₃): δ 7.43 (s, 1H), 7.29 (m, 4H), 7.06 (d, *J* = 8.5 Hz, 2H), 6.73 (d, *J* = 8.0 Hz, 1H), 4.14 (m, 1H), 2.37 (s, 3H), 1.52 (m, 3H), 1.28 (m, 5H), 0.87 (d, *J* = 6.6 Hz, 6H). LC/UV-MS analysis revealed a single UV peak at 11.19 min (~78% integrated area) with an intense ion (base peak) at *m/z* 500 (predicted mass of sodium adduct).

4.16. *N*-(1-Methylhexyl)-5-(4-chlorophenyl)-1-(2,4-dichlorophenyl)-4-methyl-1*H*-pyrazole-3-carboxamide (22)

¹H NMR (CDCl₃): δ 7.38 (s, 1H), 7.24 (m, 4H), 7.00 (d, *J* = 8.5 Hz, 2H), 6.70 (d, *J* = 8.2 Hz, 1H), 4.12 (m, 1H), 2.33 (s, 3H), 1.45 (m, 2H), 1.33 (m, 2H), 1.21 (m, 4H), 1.18 (d, *J* = 6.5 Hz, 3H), 0.83 (t, *J* = 6.6 Hz, 3H).

4.17. *N*-(1,5-Dimethylhexyl)-5-(4-chlorophenyl)-1-(2,4-dichlorophenyl)-4-methyl-1*H*-pyrazole-3-carboxamide (23)

¹H NMR (CDCl₃): δ 7.42 (s, 1H), 7.29 (m, 4H), 7.05 (d, *J* = 8.5 Hz, 2H), 6.73 (d, *J* = 8.0 Hz, 1H), 4.16 (m, 1H), 2.38 (s, 3H), 1.50 (m, 3H), 1.35 (m, 2H), 1.20 (m, 5H), 0.85 (d, *J* = 6.6 Hz, 6H). LC/UV-MS analysis revealed a single UV peak at 11.59 min (~94% integrated area) with an intense ion (base peak) at *m/z* 514 (predicted mass of sodium adduct).

4.18. *N*-(2-Ethylhexyl)-5-(4-chlorophenyl)-1-(2,4-dichlorophenyl)-4-methyl-1*H*-pyrazole-3-carboxamide (24)

¹H NMR (CDCl₃): δ 7.43 (s, 1H), 7.28 (m, 4H), 7.05 (d, *J* = 8.5 Hz, 2H), 6.94 (t, *J* = 8.0 Hz, 1H), 3.36 (m, 1H), 2.38 (s, 3H), 1.54 (m, 2H), 1.37 (m, 8H), 0.89 (m, 6H). LC/UV-MS analysis revealed a single UV peak at 11.67 min (~94% integrated area) with an intense ion (base peak) at *m/z* 514 (predicted mass of sodium adduct).

4.19. *N*-(1-Methylheptyl)-5-(4-chlorophenyl)-1-(2,4-dichlorophenyl)-4-methyl-1*H*-pyrazole-3-carboxamide (25)

¹H NMR (CDCl₃): δ 7.43 (s, 1H), 7.28 (m, 4H), 7.05 (d, *J* = 8.5 Hz, 2H), 6.73 (d, *J* = 8.2 Hz, 1H), 4.13 (m, 1H), 2.38 (s, 3H), 1.54 (m, 2H), 1.39 (m, 8H), 0.86 (t, *J* = 6.6 Hz, 3H). LC/UV-MS analysis revealed a single UV peak at 11.66 min (~93% integrated area) with an intense ion (base peak) at *m/z* 514 (predicted mass of sodium adduct).

4.20. *N*-(1-Methyldecyl)-5-(4-chlorophenyl)-1-(2,4-dichlorophenyl)-4-methyl-1*H*-pyrazole-3-carboxamide (27)

¹H NMR (CDCl₃): δ 7.42 (s, 1H), 7.28 (m, 4H), 7.05 (d, *J* = 8.5 Hz, 2H), 6.73 (d, *J* = 8.7 Hz, 1H), 4.14 (m, 1H), 2.38 (s, 3H), 1.48 (m, 2H), 1.23 (m, 17H), 0.87 (t, *J* = 7.7 Hz, 3H). LC/UV-MS analysis revealed a single UV peak at 12.64 min (~91% integrated area) with an intense ion (base peak) at *m/z* 558 (predicted mass of sodium adduct).

4.21. CBI receptor affinity and efficacy determination

All animal procedures were carried out in accordance with the Institutional Animal Care and Use Committee at the Research Triangle Institute and with the 1996 Guide for the Care and Use of Laboratory Animals as adapted and promulgated by the National Institute on

Health. Mouse vas deferens methods were performed as previously described in Ref. 28. For the competition assays utilizing rat brain membrane preparations, male CD[®] rats (Charles River Laboratories, Raleigh, NC) weighing 220–225 g were killed. The whole brains were quickly removed and placed into a 55-mL Potter–Elvehjem glass homogenizer tube maintained on ice. The methods for preparation of rat brain membranes were essentially those described by Devane et al.¹ as modified later by our laboratory.²⁷

GTP- γ -[³⁵S] assays were also performed to determine the ability of **5** and **12** to shift the binding curves of the agonists **2** or **3**. Reaction mixtures consisted of either **2** (2.5 pM to 25 μ M) to **3** (10 pM to 100 μ M), 20 μ M GDP, and 100 pM GTP- γ -[³⁵S] in 50 mM Tris–HCl, pH 7.4, 1 mM EDTA, 5 mM MgCl₂, 100 mM NaCl, and 1 mg/mL BSA. The effects of **5** and **12** on agonist binding were compared at concentrations of 1, 10, and 100 nM vs. reactions with no antagonist in a final reaction mixture volume of 0.5 mL. Binding was determined using membrane preparations as previously described.²⁸ Data analysis was performed using global nonlinear regression analysis of the dose–response curves (Prism, GraphPad), and pA₂ values were calculated. The calculations were performed with the slope of the Schild line constrained to 1, as well as unconstrained, and an *F*-test (*P* < 0.05) was used to determine the best model.

Acknowledgments

The authors thank Dr. Michael D. Walla, University of South Carolina, for the high-resolution mass spectra, and Vicki McCall for her assistance in the preparation of the manuscript. This work was supported by the National Institute on Drug Abuse (NIDA) Grant DA-19217 (B.F.T.) and NIDA Grant DA-09789 (R.G.P.).

References and notes

- Devane, W. A.; Dysarz, F. A., 3rd; Johnson, M. R.; Melvin, L. S.; Howlett, A. C. *Mol. Pharmacol.* **1988**, *34*, 605.
- Munro, S.; Thomas, K. L.; Abu-Shaar, M. *Nature* **1993**, *365*, 61.
- Matsuda, L. A.; Lolait, S. J.; Brownstein, M. J.; Young, A. C.; Bonner, T. I. *Nature* **1990**, *346*, 561.
- Abood, M. E.; Martin, B. R. *Int. Rev. Neurobiol.* **1996**, *39*, 197.
- Bouaboula, M.; Poinot-Chazel, C.; Bourrie, B.; Canat, X.; Calandra, B.; Rinaldi-Carmona, M.; Le Fur, G.; Casellas, P. *Biochem. J.* **1995**, *312*, 637.
- Howlett, A. C.; Qualy, J. M.; Khachatryan, L. L. *Mol. Pharmacol.* **1986**, *29*, 307.
- Deadwyler, S. A.; Hampson, R. E.; Mu, J.; Whyte, A.; Childers, S. J. *Pharmacol. Exp. Ther.* **1995**, *273*, 734.
- Poling, J. S.; Rogawski, M. A.; Salem, N., Jr.; Vicini, S. *Neuropharmacology* **1996**, *35*, 983.
- Mackie, K.; Lai, Y.; Westenbroek, R.; Mitchell, R. J. *Neurosci.* **1995**, *15*, 6552.
- Schlicker, E.; Timm, J.; Gothert, M. *Naunyn-Schmiedeberg's Arch. Pharmacol.* **1996**, *354*, 791.
- Szabo, B.; Dorner, L.; Pfreundtner, C.; Norenberg, W.; Starke, K. *Neuroscience* **1998**, *85*, 395.
- Levenes, C.; Daniel, H.; Soubrie, P.; Crepel, F. *J. Physiol.* **1998**, *510*, 867.
- Shen, M.; Piser, T.; Seybold, V. S.; Thayer, S. A. *J. Neurosci.* **1996**, *16*, 4322.
- Pertwee, R. G. *Pharm. Sci.* **1997**, *3*, 539.
- Le Fur, G.; Arnone, M.; Rinaldi-Carmona, M.; Barth, F.; Heshmati, H. *Abstracts of Papers*, 11th Annual Symposium on the Cannabinoids, Madrid, Spain, Jun 28–30, 2001; International Cannabinoid Research Society: Burlington, VT, 2001.
- Shim, J. Y.; Welsh, W. J.; Cartier, E.; Edwards, J. L.; Howlett, A. C. *J. Med. Chem.* **2002**, *45*, 1447.
- Thomas, B. F.; Compton, D. R.; Martin, B. R.; Semus, S. F. *Mol. Pharmacol.* **1991**, *40*, 656.
- Schmetzer, S.; Greenidge, P.; Kovar, K. A.; Schulze-Alexandru, M.; Folkers, G. *J. Comput. Aided Mol. Des.* **1997**, *11*, 278.
- Thomas, B. F.; Adams, I. B.; Mascarella, S. W.; Martin, B. R.; Razdan, R. K. *J. Med. Chem.* **1996**, *39*, 471.
- Fichera, M.; Cruciani, G.; Bianchi, A.; Musumarra, G. *J. Med. Chem.* **2000**, *43*, 2300.
- Tong, W.; Collantes, E. R.; Welsh, W. J.; Berglund, B. A.; Howlett, A. C. *J. Med. Chem.* **1998**, *41*, 4207.
- Howlett, A. C.; Mukhopadhyay, S.; Shim, J. Y.; Welsh, W. J. *Life Sci.* **1999**, *65*, 617.
- Eissenstat, M. A.; Bell, M. R.; D'Ambra, T. E.; Alexander, E. J.; Daum, S. J.; Ackerman, J. H.; Gruett, M. D.; Kumar, V.; Estep, K. G.; Olefirowicz, E. M. *J. Med. Chem.* **1995**, *38*, 3094.
- Xie, X. Q.; Eissenstat, M.; Makriyannis, A. *Life Sci.* **1995**, *56*, 1963.
- Shim, J. Y.; Collantes, E. R.; Welsh, W. J.; Subramaniam, B.; Howlett, A. C.; Eissenstat, M. A.; Ward, S. J. *J. Med. Chem.* **1998**, *41*, 4521.
- Kumar, V.; Alexander, M. D.; Bell, M. R.; Eissenstat, M. A.; Casiano, F. M.; Chippari, S. M.; Haycock, D. A.; Luttinger, D. A.; Kuster, J. E.; Miller, M. S.; Stevenson, J. I.; Ward, S. J. *Bioorg. Med. Chem. Lett.* **1995**, *5*, 381.
- Thomas, B. F.; Gilliam, A. F.; Burch, D. F.; Roche, M. J.; Seltzman, H. H. *J. Pharmacol. Exp. Ther.* **1998**, *285*, 285.
- Francisco, M. E.; Seltzman, H. H.; Gilliam, A. F.; Mitchell, R. A.; Rider, S. L.; Pertwee, R. G.; Stevenson, L. A.; Thomas, B. F. *J. Med. Chem.* **2002**, *45*, 2708.
- Pang, Y.-P.; Kozikowski, A. P. *J. Org. Chem.* **1991**, *56*, 4499.
- Loudon, G. M.; Radhakrishna, A. S.; Almond, M. R.; Blodgett, J. K.; Boutin, R. H. *J. Org. Chem.* **1984**, *49*, 4272.
- Song, Z. H.; Bonner, T. I. *Mol. Pharmacol.* **1996**, *49*, 891.
- Chin, C. N.; Lucas-Lenard, J.; Abadji, V.; Kendall, D. A. *J. Neurochem.* **1998**, *70*, 366.
- Picone, R. P.; Ayotte, L. A.; Hurst, D.; Reggio, P. R.; Khanolkar, A. D.; Fournier, D. J.; Makriyannis, A. *Abstract of Papers*, 12th Annual Symposium on the Cannabinoids, Pacific Grove, CA, July 10–14, 2002; International Cannabinoid Research Society: Burlington, VT, 2002.
- Mukhopadhyay, S.; Howlett, A. C. *Mol. Pharmacol.* **2005**, *67*, 2016.
- Williams, T. R.; Sirvio, L. M. *J. Org. Chem.* **1980**, *45*, 5082–5088.
- Seltzman, H. H.; Fleming, D. N.; Thomas, B. F.; Gilliam, A. F.; McCallion, D. S.; Pertwee, R. G.; Compton, D. R.; Martin, B. R. *J. Med. Chem.* **1997**, *40*, 3626.